IEEE Access
Multidisciplinary | Rapid Review | Open Access Journal

Received May 15, 2018, accepted June 13, 2018, date of publication June 29, 2018, date of current version July 19, 2018.

Digital Object Identifier 10.1109/ACCESS.2018.2851590

Adaptive Exponential Sliding Mode Control for a Bearingless Induction Motor Based on a Disturbance Observer

ZEBIN YANG[1], DAN ZHANG[1], XIAODONG SUN[2], (Senior Member, IEEE), AND XIAOTING YE[1]

[1]School of Electrical and Information Engineering, Jiangsu University, Zhenjiang 212013, China
[2]Automotive Engineering Research Institute, Jiangsu University, Zhenjiang 212013, China

Corresponding author: Xiaodong Sun (xdsun@ujs.edu.cn)

This work was supported in part by the National Natural Science Foundation of China under Grant 51475214, in part by the Natural Science Foundation of Jiangsu Province of China under Grant BK20170071 and Grant BK20141301, in part by the Key Project of the Natural Science Foundation of Jiangsu Higher Education Institutions under Grant 17KJA460005, in part by the Six Categories Talent Peak of Jiangsu Province under Grant 2014-ZBZZ-017 and Grant 2015-XNYQC-003, in part by the Zhenjiang Key Research and Development Project under Grant GY2016003, in part by the "333 Project" of Jiangsu Province under Grant BRA2017441, and in part by the Priority Academic Program Development of Jiangsu Higher Education Institutions.

ABSTRACT In the interest of solving the unsatisfactory control capability of a bearingless induction motor (BIM) under parameter variations, external disturbance, and load mutation, an adaptive exponential sliding mode controller and an extended sliding mode disturbance observer for on-line identification of system disturbance variables are designed. The first-order norm and switching function law is integrated into traditional reaching law, and an adaptive exponential reaching law is presented. The convergence rate can be adjusted adaptively according to the change of the sliding mode switch surface and the system state, so that the control system has the characteristics of low buffeting, excellent convergence performance, and good operation quality. In addition, the disturbance sliding mode observer takes the speed and the external disturbance of the BIM as the observation object. Meanwhile, the output of the disturbance sliding mode observer uses as the feed forward compensation for the system speed. The feedback speed can adjust operation condition adaptively with the speed error and reduce the influence of the disturbance. The simulation and experiment results indicate that the system has strong robustness to uncertainties as well as achieves the accurate identification of uncertain disturbance, the anti-disturbance ability, and the quality of operation for BIM control system can be improved, the chattering can also be inhibited simultaneously.

INDEX TERMS Bearingless induction motor (BIM), adaptive exponential sliding mode control (AESMC), disturbance sliding mode observer, anti-disturbance capacity, chattering.

I. INTRODUCTION

The bearingless induction motor (BIM) has the functions of suspension and rotation. On the basis of its specific function, the BIM can run in a special environment without friction and wear. It is widely applied to artificial heart, aeronautics and Astronautics, and high speed hard disk drive, etc [1], [2]. At the same time, the BIM integrates the two sets of polar logarithmic windings in the stator windings and breaks the magnetic field distribution of the conventional motors to realize the function of suspension and rotation. As a consequence, it has the advantages of simple structure and high mechanical strength. Nevertheless, the BIM is a complex system which has characteristics of multivariable, nonlinear and strong coupling, the requirement of controller should be improved to meet with its demands. It is especially important to design a high performance controller for the BIM disturbance compensation and speed response [3], [4].

To improve the BIM control performances, a great deal of control methods are gradually applied to the BIM control system. Sliding mode variable structure control strategy belonging to the category of modern control, according to itself state can adaptive adjust constantly [5]. It has good robustness to the uncertain constraints, internal parameter perturbation or load disturbance and imprecise mathematical models, for instance. Ultimately, the precise control of the controlled system is realized, the sliding mode variable structure control strategy shows the productive utilization prospects in control domain of AC servo system [6]–[8]. In [9], based on the

proportional switched sliding mode controller, a novel disturbance observer is designed to identify the system of rotational inertia online, which weakens the steady state error and inherent chattering phenomenon of the system. However, the differential of state variables is introduced into the dynamic sliding mode surface, and the speed differential is needed in the speed regulation system which lead to the high frequency noise, so that the speed regulation performance of the controller is further reduced. In [10], a nonlinear interference observer is used to compensate the mismatch and uncertain interferences of the system. Not only switching gain range is derived and its nominal performance is maintained, but also the system disturbance rejection capability is improved. In [11] and [12], on the basis of differential sliding surface and integral sliding surface respectively, an extended sliding mode observer is designed for the real-time observation of the internal and external disturbances with the rotation speed and the load torque as the observation object. However, these methods only consider reducing the adverse effect of the discontinuous term amplitude in the sliding mode controller and the system inherent chattering while ignoring the effects of the system inertia on the performance, so it is unable to achieve the optimum robustness. In [13], a combination of composite nonlinear feedback and integral sliding mode techniques are proposed and the synchronization errors are magnificently adjusted to the origin in the face of the perturbations, and the proposed technique achieves superior robust performance. In [5], based on the special power function and hyperbolic sine function, a reaching law is proposed, and the adaptive sliding mode control law using the counter hyperbolic sine function is also presented, the proposed method is able to effectively reduce the high frequency tremor of the input signal. However, the parameter selection is difficult and the complexity of system design on the foundation of counter hyperbolic sine function algorithm is increased. In [14], an integral sliding current control unit of fixed switch frequency is presented for a switched reluctance motor and the robustness of sliding control unit is examined. Meanwhile, the parameter constraint of the switched reluctance motor controller is derived. This method has uniform switch frequency as well as low-frequency sampling. Nevertheless, there is still a certain influence on the system speed without consideration of the large fluctuation under the external disturbance. In [15] and [16], sliding disturbance observer can be used in single winding multi phase bearingless motor and the permanent magnet synchronous motor respectively, which has better adaptability and robustness to speed and uncertain disturbances. Thus the high performance sensorless control is realized. In [17], a reaching law is proposed and applied to discrete time sliding mode control, which improves the system convergence speed effectively. In [18], to obtain superior position tracking performance control of uncertain and nonlinear time-varying systems, a novel adaptive global sliding mode control technique composed of a global sliding mode control structure and an adaptive tracker is presented.

Based on the first order norm and exponential term, an adaptive variable-rated exponential approach law which has the function of adapting sliding surface and the system state change is presented. The presented method is able to regulate reaching velocity automatically and weaken system chattering. Moreover, adaptive exponential sliding mode control (AESMC) is proposed for BIM speed control on the basis of the novel reaching law. In order to improve the anti-interference performance of sliding mode control, a disturbance sliding mode observer is designed and its output is used as the feed forward compensation of AESMC. The simulation and experimental results indicate that the presented method is able to suppress the influence of external disturbances on drive system effectively and improve the system anti-disturbance performance.

II. ADAPTIVE EXPONENTIAL SLIDING MODE REACHING LAW AND AESMC DESIGN

The nonlinear control system is considered as:

$$\begin{cases} \dot{x} = f(t,x) + b(t,x)u + g(t) \\ s = s(t,x) \end{cases} \tag{1}$$

where $x = [x_1, x_2]^T$ are status variables; $b(t,x) \neq 0$; $g(t)$ represents unsureness interference, $|g(t)| \leq \varsigma$, ς is superior limit of disturbance.

As a discontinuous on-off, the sliding mode possess the characteristics of delay and inertia in nature and makes the sliding mode exist chattering. The traditional index reaching law is designed by Gao Wei Bing and it can be adopted as [19]:

$$\dot{s} = -\varepsilon \mathrm{sgn}(s) - \lambda s \tag{2}$$

To some extent the reaching law can weaken the system inherent chattering and enhance the running worth of velocity adjusting control. However, it is a buffeting switch zone near the origin, and the coefficient ε, λ in the formula without the function of self-adjustment. The optimal convergence property cannot be achieved consequently. Based on the s and system status, a novel adaptive variable-rated exponential reaching law can be put forward to solve the above problems:

$$\begin{cases} \dot{s} = -\varepsilon \|x\|_1 e^{-\delta|s|}\mathrm{sgn}(s) - \lambda \dfrac{1}{\alpha + (1+\frac{1}{\|x\|_1} - \alpha)e^{-\delta|s|}} s \\ \lim\limits_{t\to\infty} \|x\|_1 = 0 \end{cases} \tag{3}$$

where $\|x\|_1 = \sum_{i=1}^{n} |x|$ is first order norm of the system status variable, $\lambda > 0$, $\varepsilon > 0$, $0 < \alpha < 1$, $n > 1$, $\delta > 0$.

The first order norm of the system state variables $\|x\|_1$ and the sliding mode switching function $|s|$ are introduced by the proposed reaching law. The approach speed is associated with the distance of the status variables and sliding mode switching function from the stability point. When $\|x\|_1$ keep away from $|s|$, which is known as $|s|$ is large, the status variable of the system mostly approach to $|s|$ by means of the index $-\frac{\lambda}{\alpha}s$.

At this point, the exponential term coefficient $\frac{\lambda}{\alpha}$ is greater than the coefficient λ of the traditional index reaching law. Meanwhile, the system convergence speed is accelerated by reducing α. As the status variable is capable of running to sliding surface, variable velocity term $-\varepsilon \|x_1\| \operatorname{sgn}(s)$ plays a key role. At the same time, the status enters the sliding mode surface and moves to the stable point under the action of sliding mode control, and $\|x\|_1$ decreases gradually and approaches zero, which makes $-\varepsilon \|x_1\| \operatorname{sgn}(s)$ equivalent to zero. The buffeting result from uniform velocity term $-\varepsilon \operatorname{sgn}(s)$ is weakened, and sliding motion is stabilized at the original point finally.

A sliding mode controller using first order integral sliding surface is designed, and AESMC is denoted as theorem 1.

Theorem 1: with regard to nonlinear control which presented in formula (1), s is selected as:

$$s = x_1 + c_0 \int_0^t x_1 dt \tag{4}$$

The controller can be devised as:

$$u = b^{-1}(t,x)[-f(x) - g(t) - \varepsilon \|x\|_1 e^{-\delta|s|}\operatorname{sgn}(s) - \lambda \frac{1}{\alpha + (1 + \frac{1}{\|x\|_1} - \alpha)e^{-\delta|s|}} s] \tag{5}$$

The system can converge to a steady position within a finite time, where $C = \begin{bmatrix} 1 & c_0 \end{bmatrix}$.

Stability Proof: On the basis of Lyapunov stableness theory, conditions for the existence of generalized sliding mode can be given as:

$$V = \frac{1}{2}s^2 < 0 \tag{6}$$

Combining with the formula (3), and differentiating the formula (6) with respect to time, and the parameter $1 + \frac{1}{\|x\|_1} - \alpha > 0$. Thus, $\dot{V}$ can be expressed as:

$$\begin{aligned} \dot{V} &= s[-\varepsilon \|x\|_1 e^{-\delta|s|}\operatorname{sgn}(s) - \lambda \frac{1}{\alpha + (1 + \frac{1}{\|x\|_1} - \alpha)e^{-\delta|s|}} s] \\ &= -\varepsilon \|x\|_1 e^{-\delta|s|} |s| - \lambda \frac{1}{\alpha + (1 + \frac{1}{\|x\|_1} - \alpha)e^{-\delta|s|}} s^2 < 0 \end{aligned} \tag{7}$$

Therefore, the AESMC strategy satisfies the Lyapunov stability theory, the system is guaranteed to arrive the sliding within a finite time from free position.

To verify the superiority of presented method, exponential sliding mode controller (SMC) and AESMC are designed respectively for typical nonlinear system $\begin{cases} \dot{x} = Bx + Cu + D \\ s = Ax \end{cases}$. Where, A = [2 12], $B = \begin{bmatrix} 0 & 10 \\ 0 & 0 \end{bmatrix}$, $C = \begin{bmatrix} 0 \\ -120 \end{bmatrix}$, D = [1]. The initial status variable $X(0) =$ [6 6], it is clearly can be seen from Fig.1 that AESMC possess quicker convergence velocity, buffeting is also significantly suppressed.

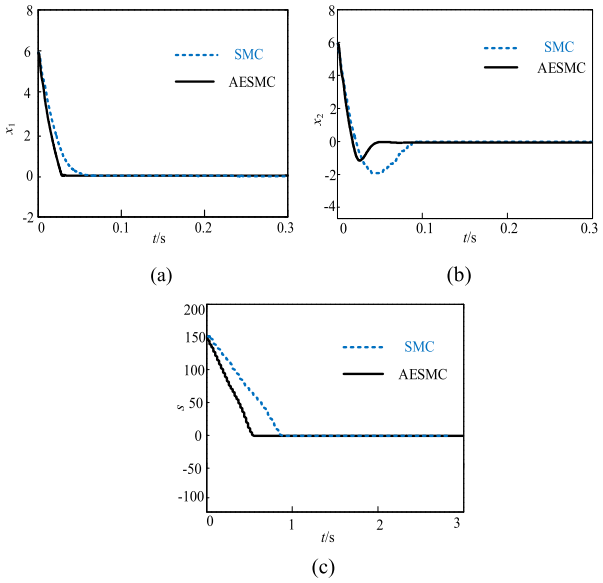

FIGURE 1. The performance comparisons of AESMC and SMC. (a) The response of x_1. (b) The response of x_2. (c) The time approach process.

III. DEVISE OF THE BIM VELOCITY USING AESMC

A. THE BIM OPTIMIZATION MODEL

Based on electromagnetic field theory, the radial suspension force under the d-q coordinate system of the BIM is expressed as [20]–[22]:

$$\begin{cases} F_x = K(i_{2sd}\psi_{1d} + i_{2sq}\psi_{1q}) \\ F_y = K(i_{2sq}\psi_{1d} - i_{2sd}\psi_{1q}) \end{cases} \tag{8}$$

where F_x, F_y are components of the radial levitation force in x and y direction; the subscript "1" on behalf of the torque winding, the subscript "2" on behalf of the suspension force winding, "s" and "r" on behalf of stator and rotor, respectively; i_{2sd} and i_{2sq} are elements of stator current of suspension force winding in d-q coordinate, respectively;. ψ_{1d} and ψ_{1q} are elements of the torque winding flux linkage in the d-$q$coordinate, respectively.

The electromagnetic torque equation is established as:

$$T_e = P_1 \psi_1 i_{qs} \tag{9}$$

The motion equation is given as:

$$T_e - T_l = \frac{J}{P_1}\frac{d\omega}{dt} \tag{10}$$

where ω represents the rotor speed; i_{qs} is components of stator current of the torque winding in q coordinate; T_e represents electromagnetic torque; T_l represents load torque; J is rotational inertia; P_1 is the logarithm of the torque winding pole.

B. THE VELOCITY DESIGN USING AESMC

The status variables are expressed as [23]:

$$\begin{cases} e_{\omega 1} = \omega^* - \omega \\ e_{\omega 2} = \int_{-\infty}^{t} e_{\omega 1} dt \end{cases} \tag{11}$$

where ω^* and ω are the given and actual velocity, respectively.

According to the formulas of (9 ∼ 11), $\dot{e}_{\omega 1}$ is given as:

$$\dot{e}_{\omega 1} = -\dot{\omega} = -\frac{P_1^2\psi_1}{J} i_{qs} + \frac{P_1}{J} T_l \tag{12}$$

In the case of parameter variations and external disturbances, $\dot{\omega}$ is expressed as:

$$\dot{\omega} = (\frac{P_1^2\psi_1}{J} + \Delta\zeta) i_{qs} - (\frac{P_1}{J} + \Delta\eta) T_l + \Delta\xi \tag{13}$$

where $\Delta\zeta$, $\Delta\eta$ and $\Delta\xi$ are corresponding to the uncertain interferences, $|\Delta\zeta| \le \upsilon_1$, $\Delta\eta \le \upsilon_2$, $\Delta\xi \le \upsilon_3$. υ_1, υ_2 and υ_3 are superior limit. Accordingly, $g_1(t)$ is regarded as the total disturbance, therefore, $\dot{\omega}$ is reduced as:

$$\dot{\omega} = \frac{P_1^2\psi_1}{J} i_{qs} + g_1(t) \tag{14}$$

where $g_1(t) = (\Delta\zeta) i_{qs} + (\frac{P_1}{J} + \Delta\eta) T_l + \Delta\xi$ and $|g_1(t)| \le \upsilon$, υ is bounded positive number. Thus, $\dot{e}_{\omega 1}$ can be expressed as:

$$\dot{e}_{\omega 1} = -\frac{P_1^2\psi_1}{J} i_{qs} - g_1(t) \tag{15}$$

The velocity error equation is described as:

$$\begin{cases} \dot{e}_{\omega 1} = -\dot{\omega} = -\dfrac{P_1^2\psi_1}{J} i_{qs} - g_1(t) \\ \dot{e}_{\omega 2} = e_{\omega 1} = \omega^* - \omega \end{cases} \tag{16}$$

When the system reaches the sliding surface, s can be expressed as:

$$s = e_{\omega 1} + c \int_0^t e_{\omega 1} dt = 0 \tag{17}$$

Differentiating the formula (17):

$$e_{\omega 1} = c_0 e^{-t/c} \tag{18}$$

From the formula (18), it can be seen that the velocity error tends to zero based on $e^{-1/c}$, so as to achieve the velocity of without overshoot tracking. Consequently, the desired sliding mode motion can be obtained by adjusting the c.

Combining of formula (16), and derivation of the sliding surface function $s = e_{\omega 1} + c \int_0^t e_{\omega 1} dt$, $\dot{s}$ can be obtained as:

$$\dot{s} = \dot{e}_{\omega 1} + c e_{\omega 1} = -\frac{p_1^2\psi_1}{J} i_{qs} - g_1(t) + c e_{\omega 1} \tag{19}$$

Combining the formula (3) and (19), it can be obtained as:

$$-\varepsilon \left\| e_\omega \right\|_1 e^{-\delta|s|} \mathrm{sgn}(s) - \lambda \frac{1}{\alpha + (1 + \frac{1}{\|e_\omega\|_1} - \alpha) e^{-\delta|s|}} s = -\frac{P_1^2\psi_1}{J} i_{qs} - g_1(t) + c e_{\omega 1} \tag{20}$$

From the formula (20), the controller i_{qs} can be designed as:

$$i_{qs} = \frac{J}{P_1^2\psi_1} \{\varepsilon \left\| e_\omega \right\|_1 e^{-\delta|s|} \mathrm{sgn}(s) + \lambda \frac{1}{\alpha + (1 + \frac{1}{\|e_\omega\|_1} - \alpha) e^{-\delta|s|}} s - g_1(t) + c e_{\omega 1}\} \tag{21}$$

The velocity controller AESMC of the BIM can be recorded as Theorem 2.

Theorem 2: with regard to the BIM rotating velocity error control which presented in formula (16), s is selected as:

$$s = e_{\omega 1} + c \int_0^t e_{\omega 1} dt \tag{22}$$

The controller i_{qs} can be designed as:

$$i_{qs} = \frac{J}{P_1^2\psi_1} \{\varepsilon \left\| e_\omega \right\|_1 e^{-\delta|s|} \mathrm{sgn}(s) + \lambda \frac{1}{\alpha + (1 + \frac{1}{\|e_\omega\|_1} - \alpha) e^{-\delta|s|}} s - g_1(t) + c e_{\omega 1}\} \tag{23}$$

Therefore, the velocity error is able to convergence toward the desired position in a finite time. The system parameters are λ, ε and α, integral constant is c.

IV. DESIGN OF DISTURBANCE SLIDING MODE OBSERVER BASED ON ON-LINE IDENTIFICATION OF DISTURBANCE INERTIA

A. THE DESIGN AND ANALYSIS OF SLIDING MODE DISTURBANCE OBSERVER

The disturbance inertia is used as an extension, and the state equation of the BIM can be expressed as:

$$\begin{cases} \dot{\omega} = \frac{P_1^2\psi_1}{J} i_{qs} + g_1(t) \\ \dot{g}_1(t) = d(t) \end{cases} \tag{24}$$

where $d(t)$ represents the rate of change of disturbance quantity $g_1(t)$.

Based on upper formula, with the motor speed and the system disturbance as the observation objects, the following disturbance expansion sliding mode observer is established as:

$$\begin{cases} \dot{\hat{\omega}} = \dfrac{P_1^2\psi_1}{J} i_{qs} + \hat{g}_1(t) + V \\ \dot{\hat{g}}_1(t) = \vartheta V \end{cases} \tag{25}$$

where $V = \gamma \mathrm{sgn}(\hat{\omega} - \omega)$; γ is the sliding mode gain; ϑ is the feedback gain; $\hat{\omega}$ and $\hat{g}_1(t)$ are the estimations of electrical angular velocity and system perturbation, respectively.

Fig.2 shows the block diagram of system disturbance extended sliding mode observer, the speed estimation error and the disturbance estimation error can be defined as:

$$\begin{bmatrix} x_1 \\ x_2 \end{bmatrix} = \begin{bmatrix} \hat{\omega} - \omega \\ \hat{g}_1(t) - g_1(t) \end{bmatrix} \tag{26}$$

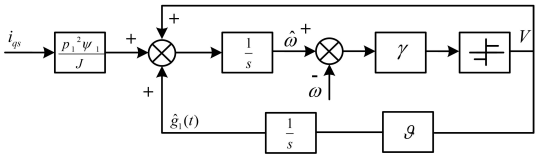

FIGURE 2. Block diagram of system disturbance extended sliding mode observer.

Formula (25) subtractive (24), the sliding mode observation error can be obtained as:

$$\begin{cases} \dot{x}_1 = x_2 + V \\ \dot{x}_2 = \vartheta V - d(t) \end{cases} \tag{27}$$

where x_1 and x_2 represents the speed and the disturbance estimation error, respectively; V represents switching function.

B. PARAMETERS SELECTION PRINCIPLE OF SLIDING DISTURBANCE OBSERVER

The observer parameters should be satisfied with the sliding mode arrival condition, and the sliding mode observation error equation (27) is brought into the (7). The arrival condition of the sliding mode can be expressed as:

$$x_1 \cdot \dot{x}_1 = x_1(x_2 + V) = x_1[x_2 + \gamma \mathrm{sgn}(x_1)] < 0 \tag{28}$$

Therefore, the parameter γ needs to be satisfied as:

$$\gamma < -|x_2| \tag{29}$$

In practical applications, the parameter γ should be selected as:

$$\gamma = -m|x_2|, m > 1 \tag{30}$$

where m is a sliding mode safety factor.

$$x_1 = \dot{x}_1 = 0 \tag{31}$$

Substituting the upper formula for the error equation (27):

$$\begin{cases} x_2 = -V \\ \dot{x}_2 = \vartheta V - d(t) \end{cases} \tag{32}$$

The upper formula is further simplified and the perturbation estimation error is obtained as:

$$x_2 = e^{-\vartheta t}\left[c + \int d(t) \cdot e^{\vartheta t} dt\right] \tag{33}$$

where c is constant. In order to make estimation error approach zero, the parameter ϑ should be chosen as:

$$\vartheta > 0 \tag{34}$$

By the formula (33), it can be seen that the convergence velocity of the perturbation estimation error x_2 is associated with ϑ.

Therefore, through parameters selection in formula (30) and (34), the system is guaranteed to convergence toward zero in a finite time, and convergence velocity can be adjusted.

C. ANALYSIS OF SLIDING MODE DISTURBANCE OBSERVER CHATTERING

As the sliding mode disturbance observer exists chattering, the chattering signal C is added to improve the estimation accuracy of the external disturbance. Formula (32) can be rewritten as:

$$\dot{x}_2 + \vartheta x_2 = \vartheta C - d(t) \tag{35}$$

Thus, the transfer function of the observation error $x_2$can be obtained as:

$$F(s) = \frac{x_2}{C - Td(t)} = \frac{1}{Ts + 1} \tag{36}$$

where the transfer function $F(s)$ is a low pass filter that can effectively suppress high frequency signals; C represents the chattering signal; T is the cycle; the cut off frequency is $\omega_c = \frac{1}{T} = \vartheta$.

From the formula (36), it can be seen that the chattering signal is filtered by low pass filter, which reduces the adverse effects of disturbance on the system control. The block diagram for vibration suppression is shown in figure 3.

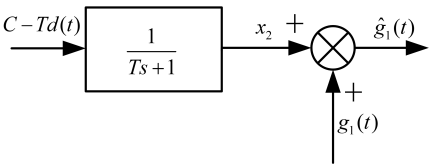

FIGURE 3. Block diagram of the observer chattering suppression.

With the feed forward compensation strategy, the disturbance sliding observer output is used as the compensation control input for system disturbance. Therefore, the BIM speed controller can be denoted as theorem 3.

Theorem 3: with regard to the BIM rotating velocity error control which presented in formula (16), s is selected as:

$$s = e_{\omega 1} + c\int_0^t e_{\omega 1} dt \tag{37}$$

The given current i_{qs} can be available as:

$$i_{qs} = \frac{J}{P_1^2 \psi_1}\{\varepsilon \|e_\omega\|_1 e^{-\delta|s|}\mathrm{sgn}(s) + \lambda \frac{1}{\alpha + (1 + \frac{1}{\|e_\omega\|_1} - \alpha)e^{-\delta|s|}} s - \hat{g}_1(t) + ce_{\omega 1}\} \tag{38}$$

From formula (23) and (38), it is clear from the formula (23) that the parameters ε and k need to be large to satisfy the change of load disturbance at the cost of increasing the amplitude of discontinuous quantity and buffeting. However, the observed disturbance quantity feedback to the given current in the formula (38), without the need of large ε and k, it can still provide the current required by the disturbance. Consequently, the system disturbance is updated in real time and the anti-disturbance capability is improved simultaneously.

V. THE VALIDATION OF SIMULATION AND EXPERIMENT

A. THE SIMULATION RESULTS AND ANALYSIS

To verify the effectiveness of AESMC and disturbance sliding mode observer for the BIM speed control system, the simulation of the BIM control system is carried out. Fig. 4 shows the system diagram of the BIM sliding mode control, and the detailed parameters are displayed in Tab. I. Setting up the difference between the speed ω^* and ω as the input, and the current value i_{qs} as the output of AESMC. The presented controller parameters are given as: $\varepsilon = c = 6$, $\lambda = 5$, $\alpha = 0.1$, $\delta = 10$, $x = e$, $m = 2$. The PI parameters can be regulated as: $k_p = 1$, $k_i = 0.001$ [24], [25].

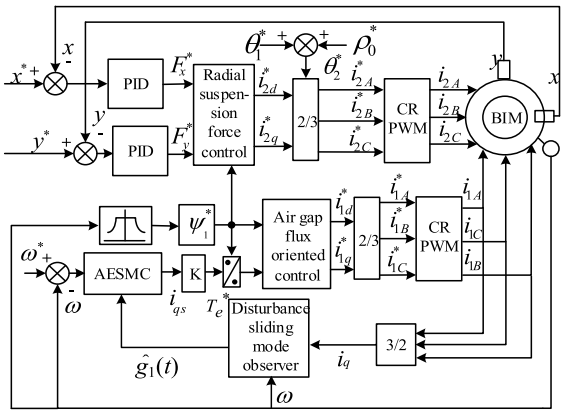

FIGURE 4. System diagram of BIM sliding mode control.

TABLE 1. The BIM parameters.

Parameters	Torque winding	Suspension winding
Stator resistance $R_s(\Omega)$	2.01	1.03
Rotor resistance $R_r(\Omega)$	11.48	0.075
Rated current I(A)	2.86	2.86
Stator and rotor mutual inductance L_m (H)	0.15856	0.00932
Stator leakage inductance L_{1sl} (H)	0.00454	0.00267
Rotor leakage inductance L_{1rl} (H)	0.00922	0.00542
Rotor mass m (kg)	2.85	2.85
Stator bore (mm)	98	98
Core length (mm)	105	105
Rotary inertia J(kg·m^2)	0.00769	0.00769
Pole pairs P	1	2

Fig. 5 shows that the system without load initiates at the given speed of 9000r/min firstly, then it operates at the stable movement when the load (3N • m) is added suddenly at the moment of $t = 0.7$s, finally, the speed mutation drops from 9000r/min to 6000r/min at $t = 1$s. As shown in Fig. 5(a), (b) and (c), when the BIM is subjected to external disturbances, the speed overshoot is larger and have

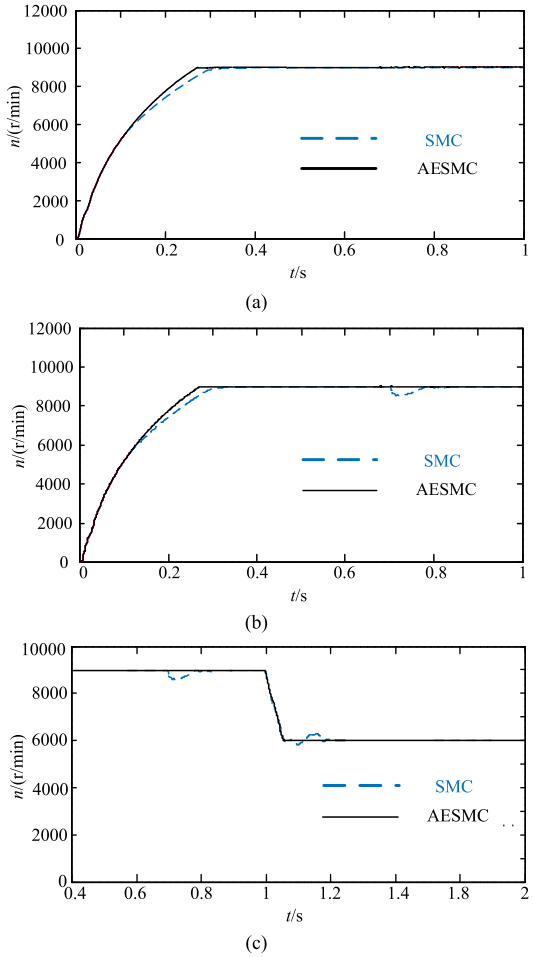

FIGURE 5. The waveforms of velocity dynamic response. (a) The velocity waveforms of the motor initiation without load. (b) The velocity waveforms of the load mutation. (c) The velocity waveforms under the torque perturbation.

a longer period of stability on the condition of the SMC strategy. While using the AESMC method, the system has faster response speed, small fluctuation and can be restored to the original value quickly. Moreover, strong anti-disturbance ability and excellent robustness can be obtained.

Fig.6 shows the simulation waveforms of current response under the conventional SMC and the proposed control strategy at the given speed of 9000r/min. It can be seen from Fig. 6(a) that the maximum value of the current under the conventional SMC is about 7A, and the final amplitude is stable on the 2A. While under the proposed control strategy, as shown in Fig. 6(b), the current shock value decreases and the final amplitude is stable at about 0.5A. It can be concluded that the AESMC control strategy with disturbance compensation can effectively reduce the current in the control loop.

Fig. 7 (a) and (b) shows the simulation waveforms of the actual load torque T_L and the observer estimation load torque $\hat{T}_L$ when the motor is stably running at 9000r/min, respectively. As shown in Fig. 7, the load (5N • m) is increased

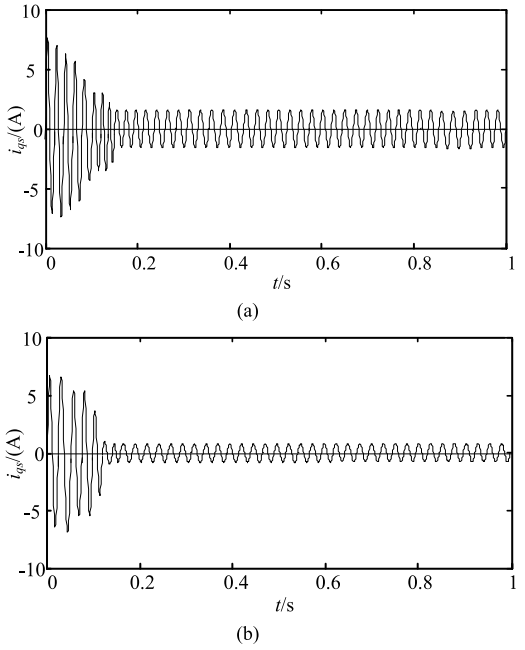

FIGURE 6. The simulation waveforms of current response. (a) The waveform of current using the conventional SMC. (b) The waveform of current using the proposed method.

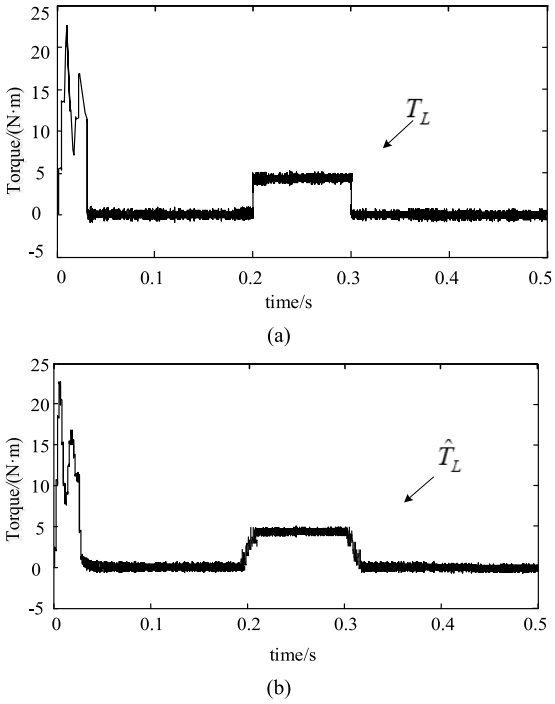

FIGURE 7. The torque waveforms under load mutation. (a) The waveform of actual torque. (b) The waveform of estimation torque.

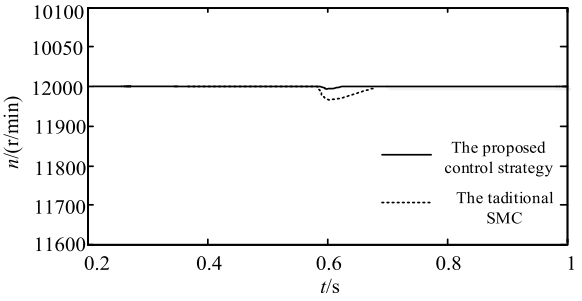

FIGURE 8. The speed response under load mutation.

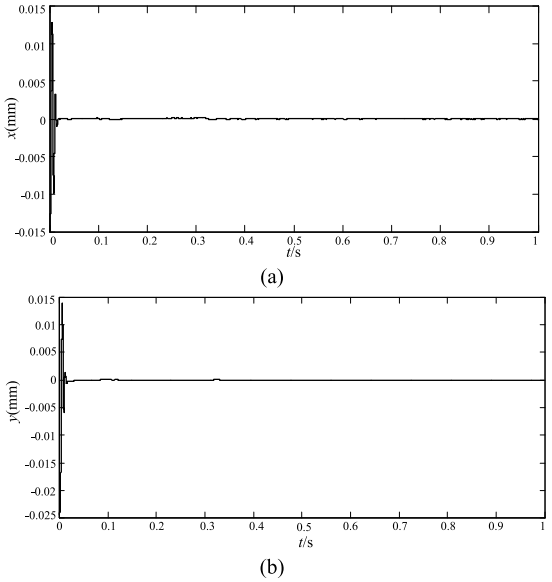

FIGURE 9. Waveforms of rotor displacement. (a) The x direction displacement. (b) The y direction displacement.

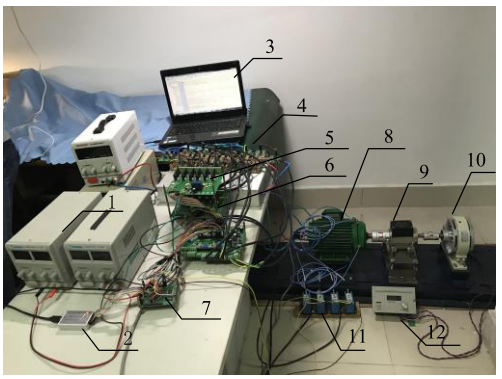

1. power 2. simulator 3. computer 4. inverter 5. suspension winding control module 6. torque winding control module 7. DSP main control board 8. BIM 9. torque sensor 10. magnetic powder brake 11. displacement sensor 12. load regulator

FIGURE 10. BIM digital experiment platform.

suddenly at the moment of $t = 0.2$s, and the load is reduced from 5N • m to no load until the moment of $t = 0.3$s. When the load changes sharply, not only the response of the system is smooth and stable, but also the observation value can quickly converge to the given value, and there is no steady state error. It can be concluded that the disturbance sliding mode observer can track the load disturbance quickly and accurately, and has strong robustness to disturbances.

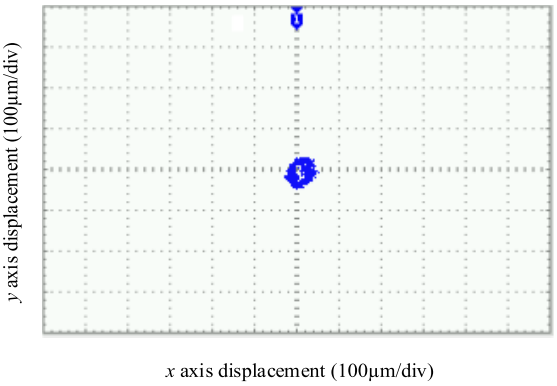

FIGURE 11. The experiment result of rotor radial displacement using the proposed method.

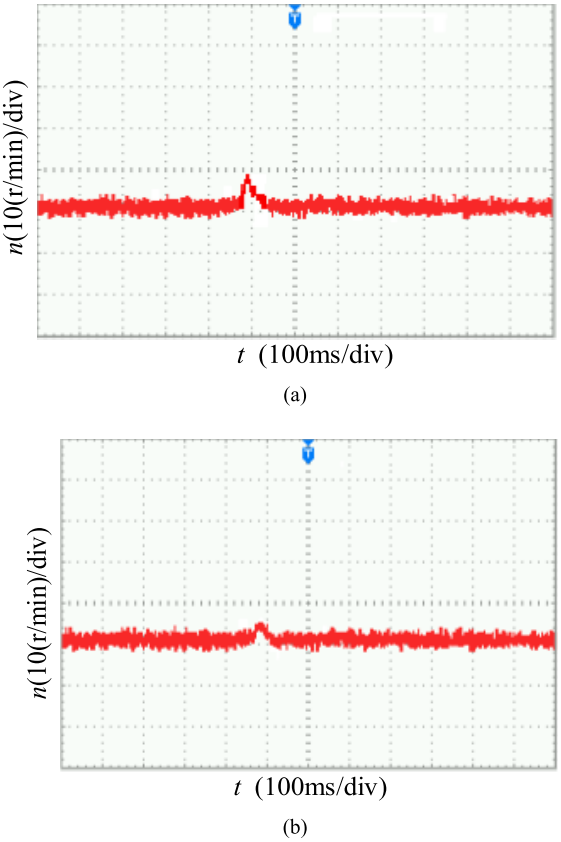

FIGURE 12. Experimental results of system dynamic response to sudden load decrease (3000r/min). (a) Velocity response of load decreases suddenly under conventional SMC. (b) Velocity response of load decreases suddenly under the proposed method.

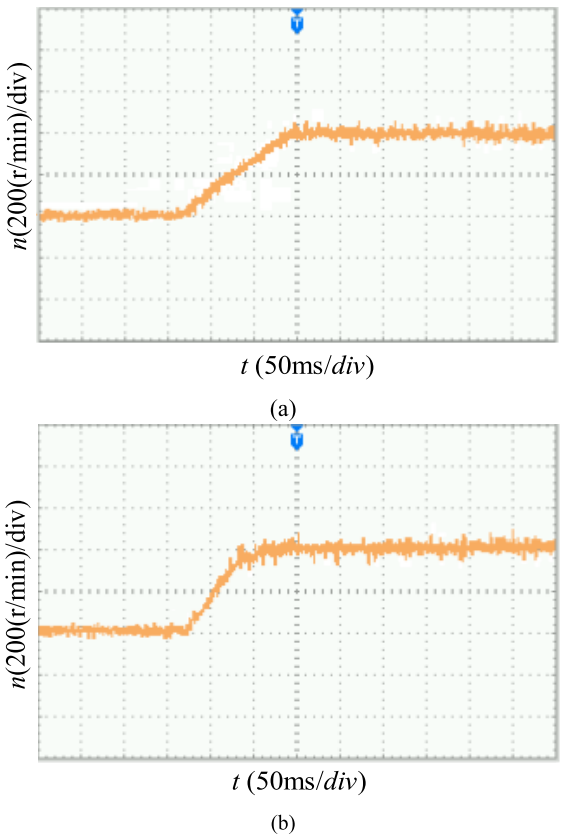

FIGURE 13. Experimental waveforms of system dynamic response to speed mutation. (a) The speed mutation using the conventional SMC. (b) The speed mutation using the proposed method.

As shown in Fig. 8, the comparison of the speed response of the motor running at 9000r/min under the proposed control strategy and the conventional SMC.As shown, the system has minimum speed fluctuation and can quickly converge to the original value under the proposed method. While under the conventional SMC the speed fluctuates greatly after the load is abrupt, and takes a long time to recover to the original speed. It can be concluded that the AESMC with the disturbance compensation control strategy has the advantages of without fluctuation of the speed and quick restore to the given value because of the real-time compensation. Meanwhile, the presented control strategy inhibits the transient fluctuation of the speed which caused by the load change effectively, and increases the disturbance resistance and stability of the system.

Fig. 9 shows the radial displacements of the method proposed at the 9000r/min in this paper. As shown,the rotor not only can quickly converge to a stable position so that fast rotation and stable suspension can be realized, but also has the excellent control performance under the proposed method with disturbance compensation control strategy.

B. THE EXPERIMENTS RESULTS AND ANALYSIS

For the sake of further verifying the availability of the presented strategy, using the BIM experimental model designed by the laboratory to build the sliding mode variable structure control system experimental platform. The TMS320F2812 control chip is used in this experiment, according to the photoelectric encoder and eddy current displacement sensor detecting the rotor speed and displacement respectively, the parameters of prototype are as the same as simulation, due to limitation of photoelectrical encoder speed measurement, the speed is set at 3000r/ min, and the auxiliary

bearing gap is 0.4mm. The whole experimental platform of the BIM is shown in Fig.10.

Fig. 11 shows the rotor trajectory diagram of the motor under the proposed method. The rotor is running around the equilibrium point and the maximum offset value is much smaller than the air gap of auxiliary bearing. It indicates that the BIM can suspend stably under the proposed strategy.

Fig. 12 shows the speed response when the load decreases suddenly under the conventional SMC and the proposed method at 3000r/min, respectively. It can be summed up as follows: Firstly, in contrast to the conventional SMC, the speed under the proposed method has quicker times and stronger security. Secondly, the velocity can be tracked rapidly and precisely. Last but not the least, the system has powerful anti-disturbance capacity and robustness.

As shown in Fig. 13, the speed mutation response under the conventional SMC and the proposed control strategy are presented from the speed 3000r/min to 3400r/min. As shown, the system speed under the proposed method has rapid responsibility and high accuracy compared with the conventional SMC.

VI. CONCLUSIONS

To achieve the capability of high dynamic response and strong resisting interference for the BIM drive system, an extended disturbance sliding mode observer is proposed based on the AESMC. The proposed strategy can automatically adjust the approaching speed of the state variable distance from the equilibrium position and suppress the chattering of the system. In addition, the extended disturbance sliding mode observer can real time estimate the system disturbance, and the output is used as the disturbance compensation, which reduces the amplitude of the discontinuous and improves the anti-interference ability of the system. The simulation and experimental results show that the proposed control strategy not only proves that the amount of interference has without effect on the performance of the control system, but also effectively improves the BIM dynamic performance and the anti-interference ability. The proposed strategy can be considered as a promising approach for controlling AC servo system. The further studies can be performed on suspension force winding control to realize tracking the given value of radial displacement quickly and accurately by means of using the AESMC.

REFERENCES

[1] X. Sun, L. Chen, and Z. Yang, "Overview of bearingless permanent-magnet synchronous motors," *IEEE Trans. Ind. Electron.*, vol. 60, no. 12, pp. 5528–5538, Dec. 2013.

[2] A. Sinervo and A. Arkkio, "Rotor radial position control and its effect on the total efficiency of a bearingless induction motor with a cage rotor," *IEEE Trans. Magn.*, vol. 50, no. 4, Apr. 2014, Art. no. 8200909.

[3] Z. Yang, F. Li, Z. Chen, and X. Sun, "Revolving speed self-detecting control based on low-frequency signal injection for bearingless induction motor," *Trans. Chin. Soc. Agricult. Eng.*, vol. 33, no. 2, pp. 41–47, 2017.

[4] X. Sun, B. Su, L. Chen, Z. Yang, X. Xu, and Z. Shi, "Precise control of a four degree-of-freedom permanent magnet biased active magnetic bearing system in a magnetically suspended direct-driven spindle using neural network inverse scheme," *Mech. Syst. Signal Process.*, vol. 88, pp. 36–48, May 2017.

[5] S. Mobayen, "Chaos synchronization of uncertain chaotic systems using composite nonlinear feedback based integral sliding mode control," *ISA Trans.*, vol. 77, pp. 100–111, Jun. 2018, doi: 10.1016/j.isatra.2018.03.026.

[6] F. Li, C. Du, C. Yang, and W. Gui, "Passivity-based asynchronous sliding mode control for delayed singular Markovian jump systems," *IEEE Trans. Autom. Control*, to be published, doi: 10.1109/TAC.2017.2776747.

[7] B. Vaseghi, M. A. Pourmina, and S. Mobayen, "Secure communication in wireless sensor networks based on chaos synchronization using adaptive sliding mode control," *Nonlinear Dyn.*, vol. 89, no. 9, pp. 1689–1704, 2017.

[8] C. Du, C. Yang, F. Li, and W. Gui, "A novel asynchronous control for artificial delayed Markovian jump systems via output feedback sliding mode approach," *IEEE Trans. Syst., Man, Cybern. Syst.*, pp. 1–11, 2018, doi: 10.1109/TSMC.2018.2815032.

[9] Y. Liu, B. Zhou, and S.-C. Fang, "Sliding mode control of PMSM based on a novel disturbance observer," *CSEE*, vol. 30, no. 9, pp. 80–85, 2010.

[10] J. Yang, S. Li, and X. Yu, "Sliding-mode control for systems with mismatched uncertainties via a disturbance observer," *IEEE Trans. Ind. Electron.*, vol. 60, no. 1, pp. 160–169, Jan. 2013.

[11] X. Zhang, L. Sun, and K. Zhao, "Sliding mode control of PMSM based on a novel load torque sliding mode observer," *Proc. Chin. Soc. Elect. Eng.*, vol. 32, no. 3, pp. 111–116, 2012.

[12] Z. Li, G. Hu, J. Cui, and G. Cui, "Sliding-mode variable structure control with integral action for permanent magnet synchronous motor," *Proc. CSEE*, vol. 34, no. 3, pp. 431–437, 2014.

[13] C. Hu, R. Wang, and F. Yan, "Integral sliding mode-based composite nonlinear feedback control for path following of four-wheel independently actuated autonomous vehicles," *IEEE Trans. Transport. Electrific.*, vol. 2, no. 2, pp. 221–230, Jun. 2016.

[14] J. Ye, P. Malysz, and A. Emadi, "A fixed-switching-frequency integral sliding mode current controller for switched reluctance motor drives," *IEEE J. Emerg. Sel. Topics Power Electron.*, vol. 3, no. 2, pp. 381–394, Jun. 2015.

[15] S. H. H. Cheng, H. Jiang, and J. K. Huang, "Position sensorless control based on sliding mode observer for multiphase bearingless motor with single set of windings," *Trans. China Electrotech. Soc.*, vol. 27, no. 7, pp. 71–77, 2012.

[16] W. Lu, H. Lin, and J. Han, "Position sensorless control of permanent magnet synchronous machine using a disturbance observer," *Proc. CSEE*, vol. 36, no. 5, pp. 1387–1394, 2016.

[17] H. Ma, J. Wu, and Z. Xiong, "A novel exponential reaching law of discrete-time sliding-mode control," *IEEE Trans. Ind. Electron.*, vol. 64, no. 5, pp. 3840–3850, May 2017.

[18] S. Mobayen and F. Tchier, "Design of an adaptive chattering avoidance global sliding mode tracker for uncertain non-linear time-varying systems," *Trans. Inst. Meas. Control*, vol. 39, no. 10, pp. 1547–1558, 2017.

[19] W. B. Gao, *Variable Structure Control Theory*. Beijing, China: China Science Technology Press, 1990, pp. 28–30.

[20] Z. Yang, L. Chen, and X. Sun, "A bearingless induction motor direct torque control and suspension force control based on sliding mode variable structure," *Math. Problems Eng.*, pp. 1–11, 2018, doi: 10.1155/2017/2409179.

[21] X. Sun, L. Chen, H. Jiang, Z. Yang, J. Chen, and W. Zhang, "High-performance control for a bearingless permanent-magnet synchronous motor using neural network inverse scheme plus internal model controllers," *IEEE Trans. Ind. Electron.*, vol. 63, no. 6, pp. 3479–3488, Jun. 2016.

[22] X. Sun, Z. Shi, L. Chen, and Z. Yang, "Internal model control for a bearingless permanent magnet synchronous motor based on inverse system method," *IEEE Trans. Energy Convers.*, vol. 31, no. 4, pp. 1539–1548, Dec. 2016.

[23] Z. Yang, D. Zhang, and X. Sun, W. Sun, and L. Chen, "Nonsingular fast terminal sliding mode control for a bearingless induction motor," *IEEE Access*, vol. 5, pp. 16656–16664, 2017.

[24] X. Zhang, L. Sun, K. Zhao, and L. Sun, "Nonlinear speed control for PMSM system using sliding-mode control and disturbance compensation techniques," *IEEE Trans. Power Electron.*, vol. 28, no. 3, pp. 1358–1365, Mar. 2013.

[25] X. Sun, L. Chen, Z. Yang, and H. Zhu, "Speed-sensorless vector control of a bearingless induction motor with artificial neural network inverse speed observer," *IEEE/ASME Trans. Magn.*, vol. 18, no. 4, pp. 1357–1366, Aug. 2013.

ZEBIN YANG received the B.Sc., M.Sc., and Ph.D. degrees in electrical engineering from Jiangsu University, Zhenjiang, China, in 1999, 2004, and 2013, respectively. From 2014 to 2015, he was a Visiting Scholar with the School of Electrical, Mechanical, and Mechatronic Systems, University of Technology Sydney, Sydney, Australia. He is currently a Professor with Jiangsu University. His main research interests include drives and control for bearingless motors and magnetic levitation transmission technology.

DAN ZHANG was born in Suzhou, Anhui, China, in 1992. She is currently pursuing the master's degree with Jiangsu University. Her main research interest is optimal design and intelligent control of bearingless motors.

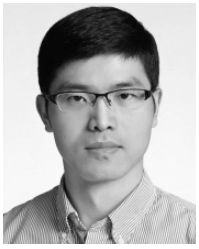

XIAODONG SUN (M'12–SM'18) received the B.Sc. degree in electrical engineering, and the M.Sc. and Ph.D. degrees in control engineering from Jiangsu University, Zhenjiang, China, in 2004, 2008, and 2011, respectively.

Since 2004, he has been with Jiangsu University, where he is currently a Professor with the Automotive Engineering Research Institute. From 2014 to 2015, he was a Visiting Professor with the School of Electrical, Mechanical, and Mechatronic Systems, University of Technology Sydney, Sydney, Australia. His current teaching and research interests include electrical machines and drives, drives and control for electric vehicles, and intelligent control. He has authored or coauthored over 80 refereed technical papers and one book, and he is the holder of 36 patents in his areas of interest.

XIAOTING YE was born in Huai'an, Jiangsu, China, in 1981. She received the B.S. and M.S. degrees from the China University of Mining and Technology in 2003 and 2006, respectively. She is currently pursuing the Ph.D. degree with Jiangsu University. Her main research interests include electric drive and nonlinear intelligent control of motors.